Structure and Function of Chihuahuan Desert Ecosystem
The Jornada Basin Long-Term Ecological Research Site
Edited by: Kris Havstad, Laura F. Huenneke, William H. Schlesinger
Chapter 7. Abrahams, A.D., Neave, M., Schlesinger, W.H. et al. 2006

Submitted to Oxford University Press for publication
ISBN 13 978-0-19-511776-9

Structure and Function of Chihuahuan Desert Ecosystem
The Jornada Basin Long-Term Ecological Research Site
Edited by: Kris Havstad, Laura F. Huenneke, William H. Schlesinger
Chapter 7. Abrahams, A.D., Neave, M., Schlesinger, W.H. et al. 2006

7

Biogeochemical Fluxes across Piedmont Slopes of the Jornada Basin

Athol D. Abrahams, Melissa Neave, William H. Schlesinger, John Wainwright, David A. Howes, and Anthony J. Parsons

This chapter is an overview of recent studies of the movement of water, sediment, and nutrients across a principle piedmont slope, or bajada, of the Jornada Basin. Bajadas are extensive, gently sloping surfaces formed by the coalescence of alluvial fans and are a major landscape component of the basin and range province (see chapter 2, figures 2-3 and 2-6). Over the past four decades a considerable body of research has elucidated the form and function of alluvial fans (Bull 1977; Blair and McPherson 1994; Harvey 1997), but less attention has been paid to bajadas. In particular, the bajadas most neglected are those where channels converge and diverge at irregular intervals downslope. This type of bajada is found at the base of Summerford Mountain, the northernmost peak of the Dona Ana Mountains on the western edge of the Jornada Basin (see chapter 2, figure 2-5b). For convenience, this bajada is hereafter referred to as the Summerford bajada. The research has involved rainfall simulation experiments on small plots, monitoring of two small watersheds on this bajada, and computer modeling of the processes operating in these watersheds and over the bajada as a whole. A detailed understanding of the hydrology and hydraulics of overland flow on this bajada requires a numerical model of the rainfall-runoff process. The objective of this chapter is to detail the model and draw conclusions from model simulations about hydrologic transports of sediment and nutrients across this bajada. Because these piedmonts are important surfaces in this desert (chapter 2) an understanding of their hydrologic and biogeochemical dynamics is crucial to understanding landscape dynamics in the basin and throughout arid regions.

The Summerford Bajada

Geology and Soils

Summerford Mountain is a steep-sided, rocky inselberg (i.e., isolated mountain) that rises 380 m above the surrounding bajada to an elevation of 1,780 m. The mountain is composed of

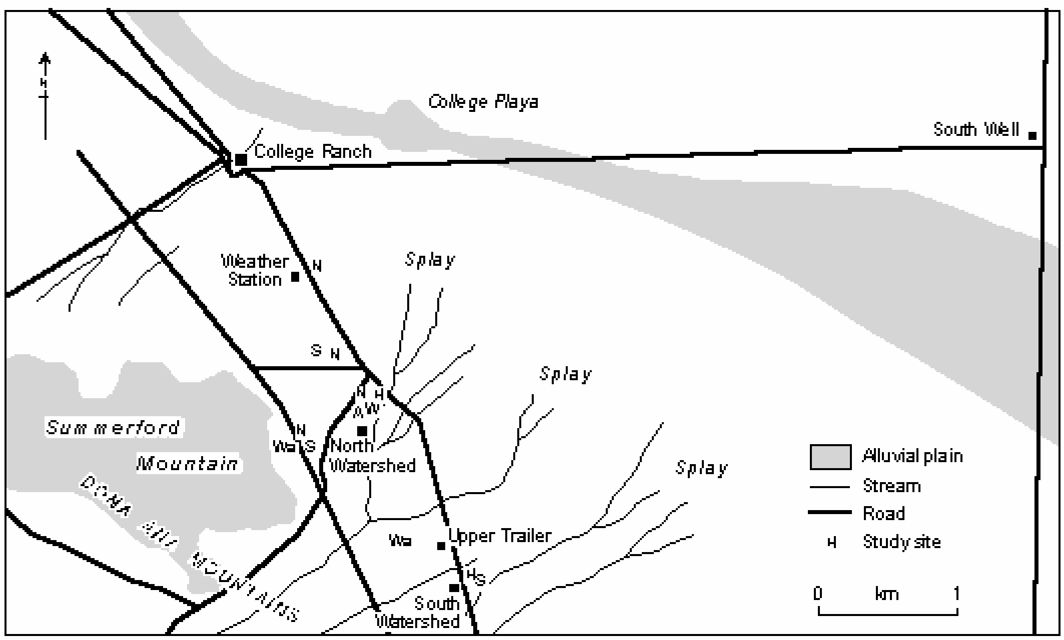

Fig. 7-1. Map of the study area showing the locations of the field experiments reported by Abrahams et al. (2003) (A), Howes and Abrahams (2003) (H), Neave and Abrahams (2001; 2002) (N), Schlesinger et al. (1999; 2000) (S), Wainwright et al. (1999a) (W), and T.J. Ward (Wa).

monzonite porphyry of Oligocene age (Seager et al. 1976) and has a fringing bajada on its northern and eastern sides. This study focuses on the bajada to the east, which extends 2.5 km to the basin floor (figure 7-1) at an average gradient of 4%.

The soils on the upper bajada at the base of Summerford Mountain are Mollisols or, more specifically, Torriorthentic Haplustolls (chapter 4). The surface horizon is a sandy loam (79%

sand, 13% silt, 8% clay) with an abundance (> 30%) of fine to medium quartz pebbles weathered from the monzonite. Downslope a calcite-rich paleosol is exposed over a limited area. This soil is classified as a Typic Haplocalcid. The caliche horizon is at or just below the surface, so infiltration rates are low and shrubs are small. Over the remainder of the bajada the soils are Typic Haplargids. The surface horizon has a sandy loam or loamy sand texture (70–85% sand, 10–20% silt, 5–10% clay) and contains variable amounts of gravel, which become concentrated on the surface as an erosional lag. The gravel cover increases from 5% to > 80% from northwest to southeast across the bajada (figure 7-1). The Typic Haplargids become finer down the bajada with the surface horizon having a loamy texture (64% sand, 24% silt, and 11% clay) adjacent to the basin floor. Scattered across the lower bajada are large poorly defined areas of undifferentiated sandy sediments or Entisols that have been deposited by the sandy washes splaying out over the surface.

Vegetation

Vegetation surveys (chapter 10, figures 10-1 and 10-2) indicate that prior to 1915 the Summerford bajada was covered with black grama (*Bouteloua eriopoda*) grasses (Buffington and Herbel 1965). Today, a grassland community is found only on the Mollisols at the base of Summerford Mountain. The community is dominated by bunch grasses, notably black grama, treeawn (*Aristida*) species, and Lehmann lovegrass (*Eragrostis lehmaniana*), an exotic introduced to control erosion along the power line that crosses the bajada. In the middle of the bajada a shrubland community dominated by creosotebush (*Larrea tridentata*) is well established (Stein and Ludwig 1979). Creosotebush extends to the bottom of the bajada, where tarbush (*Flourensia cernua*) replaces it as the dominant shrub on the finer-textured soils. North and east of Summerford Mountain, degraded grassland covers the lower part of the bajada. In the grasslands about 40% of the ground surface is bare, but this percentage is closer to 70% in the degraded grassland, which is believed to represent the transition from grassland to shrubland. Both the creosotebush shrubland and the degraded grassland are underlain by soils with a subsurface argillic horizon. The presence of all three vegetation communities in close proximity to one another was a major reason for selecting this particular area for study.

Surface Crusts and Animal Disturbance

The Summerford bajada is characterized by the widespread development of surface crusts. These crusts consist of a thin surface layer 1–3 mm thick that is both stronger and less permeable than the underlying soil. The crusts may be either physical or biological in character. Most biological crusts in the study area are due to the presence of filamentous cyanobacteria. Crusts of this type cover much of the ground surface in the shrubland and degraded grassland but are patchier in the grassland. They are best developed where the soil surface is relatively moist, such as under shrubs and grasses, though their distribution is quite uneven. They are least developed where erosion rates are relatively high, such as in rills.

In contrast to biological crusts, physical crusts form when raindrop impact blocks soil pores by compressing the soil surface and/or by entraining clays that then get carried into the pores by infiltrating water (McIntyre 1958; Moore 1981; Kidron et al. 1999). Physical crusts often develop where biological crusts have been disrupted. Cyanobacteria may recolonize a disturbed area within two years and reach their predisturbance biomass within five years (Kidron personal communication). In the meantime, a physical crust may form during a single storm where the soil is suitable. Poesen (1992) showed that the optimal soil textures for the development of physical crusts are sandy loams and loamy sands. These textures are found in the surface soils over most of the bajada. As a result, physical crusts develop readily in these soils and have a major impact on surface runoff.

Another distinctive feature of the Summerford bajada is the degree to which the ground is disturbed by faunal activity. Small mammals are largely responsible for this disturbance. These animals dig and scratch the soil in search of food (plant stems, roots, seeds, and insects). The resulting holes are typically 20–30 mm deep but may have depths of 200 mm. In addition, there are burrows of indeterminate depth and extent. Following a storm, the animals dig up the surface until the next storm obliterates their diggings. In as much as digging disrupts the surface crust (both physical and biological) and scatters loose sediment over the ground surface, it might be expected to have a profound effect on the movement of water and materials across the bajada, particularly in the degraded grassland and shrubland (Neave and Abrahams 2001).

Drainage

Runoff on the bajada surface arises both from infiltration-excess rainfall on the bajada itself and from sand-bedded streams issuing from Summerford Mountain that debouch onto the head of the bajada. All sand-bedded streams eventually splay out over the bajada surface, and their flow becomes dispersed. The smaller of these streams terminate within the grassland community at the base of Summerford Mountain, whereas the larger ones survive to the lower bajada. The latter streams have alternating single-channel and multichannel reaches that are equivalent to Bull’s (1997) “discontinuous ephemeral streams.” Along the channel margins are frequent mesquite (*Prosopis glandulosa*) and white thorn (*Acacia constricta*) shrubs. The splays of these channels are typically grassy and elevated a meter or so above the bajada surface.

Infiltration-excess runoff is highest in the shrubland and concentrates downslope to form an extensive network of rills. These rills generally head within 5 m of the local divide, and like the larger sandy washes, they have alternating single- and multichannel reaches. Elsewhere, the multichannel reaches are replaced by reaches with no clearly defined channelized flow that are herein called beads because they are reminiscent of beads spaced out along a necklace. At their upstream end they are similar to the splays of the larger sand-bed streams. However, they differ at their downstream end, where their flow coalesces into a single channel. Although the sequences of beads and single-channel reaches tempts one to think of them as coherent hydrological units, the functional relationship between a bead and the downstream channel is unclear. An alternative view is that a bead is equivalent to a sand splay on one of the larger sand-bed streams and that the single-channel reach at the bead's downstream end is a hydrologically independent unit that forms as a result of the concentration of infiltration-excess runoff downslope of the bead. The single-channel reaches are typically less than 2 m wide and incised into the bajada surface by as much as 0.8 m. Apart from their uppermost reaches, these reaches are characterized by sandy beds.

In the grassland, the rills are smaller (typically 0.3 m wide) and more widely spaced (about 20 m) than in the shrubland, and they do not form an integrated network. Instead, individual rills extend downslope for 15–20 m before they dissipate, choked by grass and deposited sediment. In the degraded grassland, rills are rare and virtually all drainage is inter-rill.

Ground Surface

In inter-rill areas, the nature of the ground surface is strongly influenced by the vegetation. Thus in the grassland the ground surface is characterized by large clumps of grass, which give rise to a pronounced microtopography with an amplitude of about 0.2 m and a wavelength of about 0.5 m. The degraded grassland, which is found on the gentler slopes of the lower bajada, has smaller and more widely spaced clumps of grass and an almost planar ground surface between the clumps. As a result, the microtopography has amplitude of no more than 0.1 m and a wavelength of 0.25–0.5 m. Surface runoff in the grassland and degraded grassland is clearly dispersed by the grass. Although there are obvious threads of flow and features that resemble small rills (termed “prerills” by Roels 1984), they rarely persist over distances greater than 5 m. In the degraded grassland, the microtopography is subdued and threads of flow are difficult to follow.

In contrast, in the shrubland the inter-rill areas are characterized by broad, shallow swales stretching between mounds topped by shrubs. The microtopography has amplitude of about 0.10 m and a wavelength ranging from 1.5 to 3 m. The mounds grow, at least initially, as fine sediments are deposited beneath shrub canopies by eolian and/or rainsplash processes (Carson and Kirkby 1972; Parsons et al. 1992). Once developed, the mounds divert surface runoff into intershrub areas where it may erode the surface sufficiently to form a rill. Where there is a significant proportion of gravel in the surface soil, a gravel lag accumulates in intershrub areas and impedes erosion in general and rill formation in particular.

Modeling Runoff Events

Howes and Abrahams (2003) developed an event-based, two-dimensional runoff model to simulate overland flow within two small shrubland watersheds—north watershed (figure 7-2a) and south watershed (figure 7-2b)—and made detailed field surveys of these watersheds using a total station. The principal difference between the watersheds is that south watershed is incised about 1 m below the general surface of the bajada and has a surface gravel cover that averages about 30%. North watershed is not incised and is largely free of surface gravel. Both watersheds have gradients of about 4%. In the model, grids of 1 m × 1 m cells, in which each cell is classified as either intershrub or shrub, represent the watersheds. The rills are treated as intershrub surfaces. Flow is routed from cell to cell by numerically solving the two-dimensional kinematic wave equation using a predictor-corrector, finite-difference scheme (Davis 1988). The flow velocity is computed using the Darcy-Weisbach flow equation, and infiltration is computed using the Smith-Parlange equation (Smith and Parlange 1978). Parameter values were obtained for the shrub and intershrub surfaces in each watershed from rainfall simulation experiments and a field survey. Rainfall data were provided by tipping bucket rain gauges located adjacent to the outlets of the watersheds where flow discharge was recorded at calibrated supercritical flumes. Such flumes are designed to accelerate the flow as it passes through, thereby ensuring that there is no deposition on the floor of the flume that might corrupt the stage-discharge rating curve. Figure 7-3 shows simulated and observed hydrographs for the two watersheds for a storm on July 30, 1997. In the initial simulations, the model underpredicted the runoff from both watersheds as a result of overpredicting the saturated hydraulic conductivity K_s.

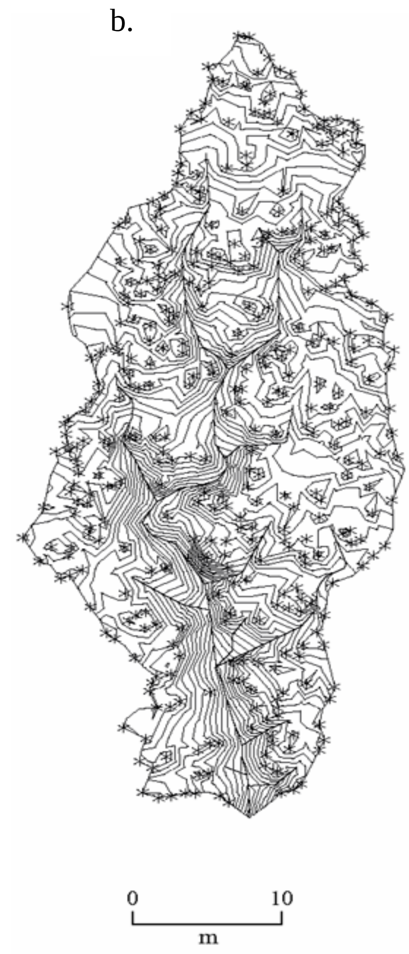

Fig. 7-2. Maps of (a) north and (b) south watersheds. The contour interval is 5 cm. Shrub locations are indicated by asterisks.

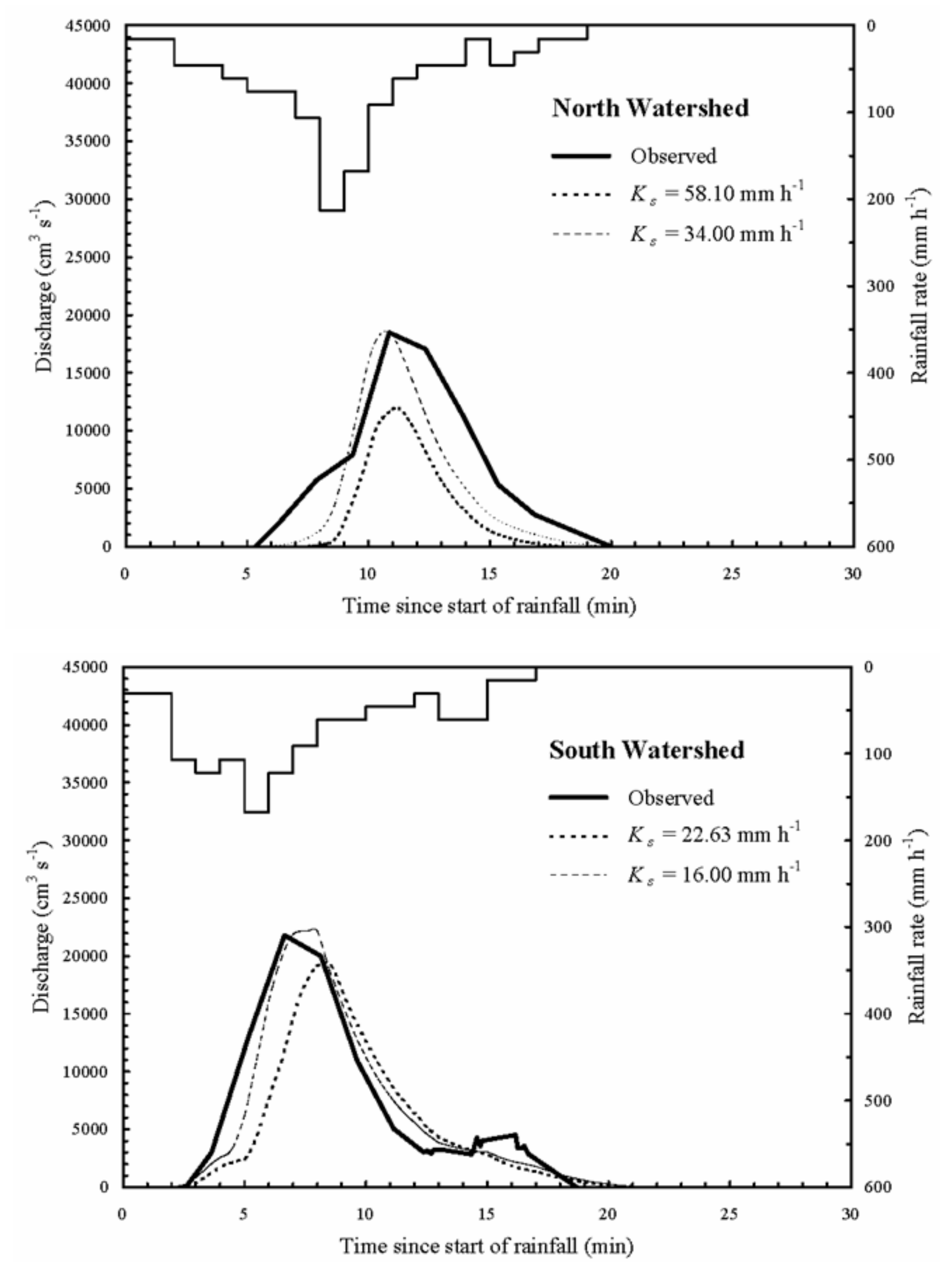

Fig. 7-3. Simulated (K values) and observed (measured) hydrographs for the July 30, 1997, storm in (a) north watershed and (b) south watersheds.

This overprediction is presumed to be due to the surface crust in intershrub areas being better developed at the time of the storm than at the time of the rainfall simulations, that is, late June when the crust was degraded by animal activity. Model performance was improved by reducing the intershrub K_s values to account for the crusting (Moore 1981; Bosch and Onstad 1988; Rawls et al. 1990). The second pair of simulated hydrographs shown in figure 7-3 was generated by reducing the intershrub K_s from 58.10 mm/h to 34.00 mm/h for the north watershed and from 22.63 mm/h to 16.00 mm/h for the south watershed. The relative reduction in K_s is less for south watershed because gravel on intershrub surfaces promotes runoff and at the same time renders the soil less susceptible to crusting than the north watershed intershrub surface that is free of gravel. Given that the formation of a physical crust has the potential to alter the infiltration characteristics of a watershed from storm to storm, more work is required to develop a procedure for estimating the development and destruction of surface crusts and their effect on K_s for individual rainfall events.

The 2D model provides an investigative tool that can be used to study the hydrologic processes operating in shrubland ecosystems. For example, field studies have indicated that lateral movements of water and nutrients are important in desert ecosystem function (Schlesinger and Jones 1984; Noy-Meir 1985), but the lack of a detailed runoff model has meant that a quantitative investigation of lateral movement of water and nutrients at the scale of the individual shrub has not been possible. Howes and Abrahams (2003) demonstrated how their 2D model could be used to model the lateral movement of water at this scale.

Using the 2D model, Howes and Abrahams (2003) conducted a study of the relative importance of run-in infiltration (i.e., infiltration of overland flow in a cell whose infiltration capacity has not been satisfied) and rainfall infiltration (i.e., infiltration of rain falling directly into a cell containing a shrub) in supplying water to shrubs. Wet and dry antecedent soil moisture conditions in each watershed were simulated for a range of rainfall conditions typical of the bajada. Model cells were assigned a value of K_s at random from a log normal distribution to represent spatial variability in infiltration. The mean and coefficient of variation of the distribution were based on the data from the rainfall simulation experiments that were conducted to parameterize the model. The simulation results were expressed in terms of the mean run-in percentage, which is the depth of run-in infiltration expressed as a percentage of the total depth of infiltration in a cell.

It was found that the mean run-in percentage for all shrub cells varied with mean rainfall rate in a similar manner in both watersheds (figure 7-4).

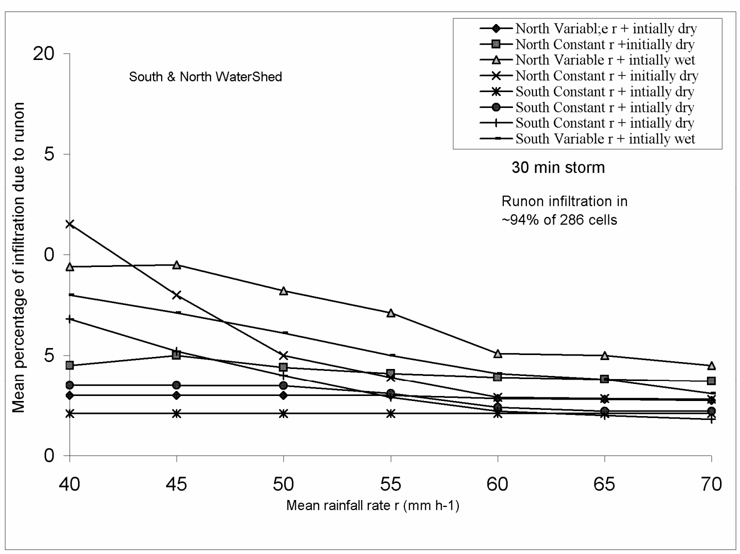

Fig. 7-4. Graph of mean percentage of infiltration due to runon against mean rainfall rate for all shrubs in north and south watersheds predicted by the 2D model. In the north watershed, run-on infiltration occurred in 98 percent of shrub cells and accounted for 3 to 12 percent of the total infiltration under shrubs. In the south watershed, run-on infiltration occurred in 94 percent of shrub cells and accounted for 2 to 8 percent of the total infiltration under shrubs

The highest mean run-in percentages were associated with an initially wet soil, a temporally variable rainfall pattern, and low rainfall rate. Run-in infiltration was slightly more important in north watershed, being equal to 3–12% of the total infiltration, compared to 2–8% for south watershed. This difference was attributed to both the higher values of K_s and the lower shrub mounds in the north watershed (figure 7-2). The computed mean run-in percentages are sufficiently large to suggest (1) that lateral flows must be taken into account in studies of shrubland ecosystems and (2) that a much broader study of the role of run-in infiltration in supplying water to shrubs would be worthwhile.

Transmission Losses

The ability of ephemeral channels to carry water and sediment depends, among other things, on transmission losses through their beds. In our investigation of transmission losses in the discontinuous channels on the bajada surface, we have so far examined only the rills in the shrubland community. This examination has been conducted on both single-channel reaches and on a bead. Sedimentological analysis of the beds of single-channel shrubland rills and sandy washes reveal a similar structure. The top 30 cm consists of loose, coarse sand and gravel below that is a finer, more indurated layer. This sedimentological similarity suggests that the transmission losses of the sandy washes may not be dissimilar to those measured in the rills.

Rills

Experiments were conducted on 10 rill reaches (Parsons et al. 1999). Water simulating rill flow was introduced at the upper end of each reach, and the outflow from the reach was measured by taking timed volumetric samples. Transmission losses at equilibrium averaged 9.24 mm/min, which is about an order of magnitude greater than final infiltration rates measured in bare inter-rill areas between shrubs. This difference may be due to several factors, the most likely being that surface sealing occurs in inter-rill areas but not in the rills and hydraulic heads are greater in rill flow than in inter-rill flow.

Support for the notion that hydraulic head accounts for greater infiltration loss in the rills is obtained from estimates of downstream changes in discharge through the rill reaches. These estimates were made by measuring depth and width of flow at four cross-sections within the rill reaches and assuming uniform velocity throughout the reach. Figure 7-5 shows the pattern of discharges obtained from these measurements.

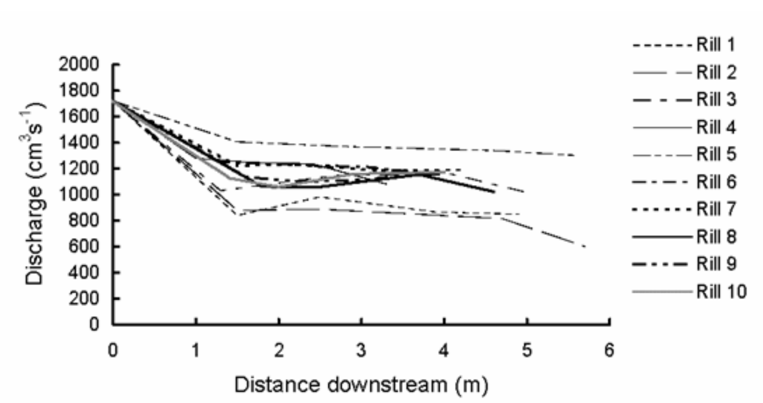

Fig. 7-5. Rill discharge as a function of flow distance for 10 rills in the shrubland community of the Summerford bajada study area.

The pattern is clearly nonlinear and shows that transmission loss decreases downhill as the hydraulic head decreases. This pattern implies that where rill flow extends beyond the spatial limits of the generating storm, most of the flow will be lost through the bed close to the edge of the storm.

Beads

The significance of beads for runoff from the bajada has been investigated using supercritical runoff flumes to monitor discharges in natural events. Three flumes were installed in north watershed and three in south watershed (figure 7-1). In south watershed, flumes were set up on two tributary rills, and a third flume was set up just downstream of their confluence. All rills consist of a single channel. The contributing areas for these flumes are 889.7, 431.3, and 1,833.9 m^2. In contrast, north watershed contains two tributary channels that feed into a bead. Flumes were installed on these rills, just upstream of the bead. A third flume was installed just downstream of the point where a clearly defined channel emerges from the bead. The contributing areas for these flumes are 775.2, 3,379.3, and 5,936.1 m^2. Serendipitously, the ratio of the sum of contributing areas of the two upstream flumes to the downstream flume is 1.4 in both cases. The flumes are equipped with stilling wells that record maximum depth of flow in a storm event. Using the ARS calibration for the flume design (Smith et al. 1981), these depths were converted to peak discharges.

Between January 26, 1995, and July 28, 1997, 49 rainfall events were recorded in north watershed and 45 in south watershed. Of the rainfall events in north watershed, runoff was recorded on 18 occasions in one or both of the upstream flumes and on 12 occasions in the downstream flume. For south watershed, the respective figures are 17 and 11 occasions. Whereas those events that were recorded upstream but not downstream in the south watershed are typically of very small magnitude (< 850 cm^3/s); in north watershed, the threshold is much greater (> 26,200 cm^3/s). This difference reflects the high infiltration capacity of the bead in north watershed.

Figures 7-6a and 7-6b show the relationships for north watershed and south watershed between peak discharge at the watershed outlet and the sum of the peak discharges from the two tributaries. Assuming that the peak discharge is a reasonable surrogate for total discharge, in both north and south watersheds the ratio of the output to the sum of the inputs might normally be expected to be approximately 1.4 (the ratio of the sum of the tributary areas to the entire watershed area). However, given the values for transmission losses just reported, a more reasonable ratio might lie between 1.1 and 0.7. For the single channels of south watershed, most ratios are within or above this range, and only at very small discharges is this not the case (figure 7-6a). Discounting these very small discharges, there is no clear relationship between the ratio of output to input and the input discharge. In contrast, in north watershed two-thirds of the observed ratios fall below 0.7, and there is a clear trend for the ratio to increase with discharge (figure 7-6b). This result suggests that the bead is absorbing water well in excess of the transmission losses in single channels. Thus beads appear to be important sinks for water on the bajada and, consequently, also for sediments and nutrients. The ecological importance of these sinks needs further investigation.

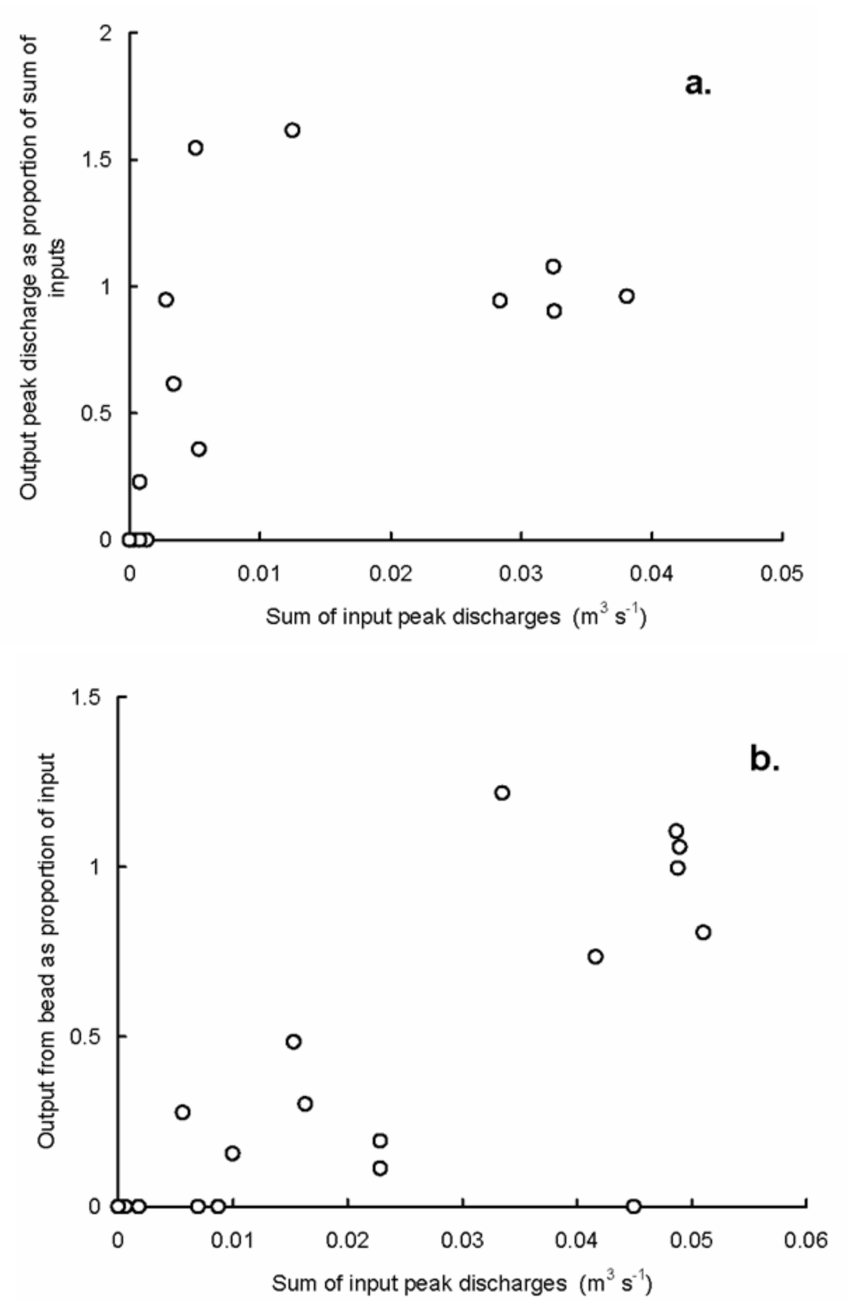

Fig. 7-6. Comparison of peak inflow and outflow discharges for (a) south watershed and (b) north watershed for runoff events between January 16, 1995 and July 28, 1997-

Synthesis: Modeling Bajada Hydrology

To extrapolate results from plot experiments to the overall bajada scale, a series of numerical simulations has been carried out. The model used is based on that developed by Scoging (1992) and Parsons et al. (1997). Overland flow is generated using a Hortonian infiltration-excess method, based on the Smith and Parlange (1978) model, to allow for moisture storage. This technique allows for run-in infiltration that affects the amount of moisture available to plants in the bajada soils. Flow routing uses the steepest descent method based on the topography, and flow rating is calculated using the Darcy-Weisbach friction factor.

Input data for the model are derived from a number of sources. The topography is derived from the 30-m digital elevation model (DEM) produced from the 1:24,000 maps from the U.S. Geological Survey (USGS). The model was run on the extract of the USGS 30-m DEM that covers the bajada area to the north and east of Summerford Mountain. Infiltration and friction factor parameters for the model were distributed according to the spatial distribution of the vegetation communities present on the bajada, using measurements derived from the field experiments already described. The presence of rills is accounted for by weighting the infiltration rates and friction factors according to the mean rill area in the cells belonging to different vegetation types. The infiltration-weighting factor is by the rate of transmission loss and the friction factor weighting according to measured values from rills at Walnut Gulch (Abrahams et al. 1996). The storm illustrated occurred between 15:59 and 16:15 on July 30, 1997. The total rainfall at the north watershed was 19.6 mm, with 1-minute intensities ranging from 15 to 167.4 mm/h.

The results of the model simulation were different patterns in resultant soil moisture according to the different habitats. Summerford Mountain itself had the lowest soil moisture values because of rapid runoff. On the degraded grassland, the predicted soil moisture clearly followed the gradient of the storm cell, suggesting little connectivity down the bajada. There was a distinctive break between the degraded grassland and the shrubland area. The shrubland had more diffuse down-bajada changes in soil moisture and lower soil moisture values for equivalent rainfall. Both of these were the result of the higher runoff rates on the shrubland and suggested that the shrubland is spatially more interconnected. It is difficult to reach firm conclusions about the grassland because it occupies such a small zone at the foot of Summerford Mountain, although it seems to behave in the same way as the degraded grassland. Overall, the results suggest that both the spatial pattern of the rainfall cell and the location of the different habitats control the spatial redistribution of soil water on the bajada.

Sediment

The initial focus of this project was on inter-rill areas because the movement of water, sediment, and nutrients begins in these areas. Although our studies are beginning to shift to the scale of small watersheds, rills, and sandy washes (Parsons et al. 1999; Howes and Abrahams 2003), the study of sediment and nutrient transport continues at the inter-rill scale (Schlesinger et al. 1999, 2000; Neave and Abrahams 2001, 2002). Consequently, the remainder of this chapter examines the processes and controls of sediment and nutrients at the intershrub scale.

Detachment and Transport

Soil erosion involves both the detachment and removal of soil particles. In inter-rill areas, detachment is accomplished predominantly by raindrops. Where overland flow depth is less than about three raindrop diameters (Kinnell 1991), raindrops falling at terminal velocity are capable of splashing particles with diameters up to 12 mm in all directions (Kotarba 1980). The trajectories of such particles are longer in the downslope direction, so there is a net downslope flux with the rate proportional to the sine of the slope. The rate of splash transport decreases as overland flow becomes deeper, and it decreases as vegetation, litter, and gravel covers increase. Owing to the scarcity of vegetation, splash transport is generally more important in desert landscapes than in humid ones. Nevertheless, it remains a relatively minor transport process, accounting for only 5–25% of the sediment transported by overland flow (Abrahams et al. 1994).

The main role of rainfall is to detach or loosen soil particles and lift them into the flow, which then transports them downslope. Raindrops not only loosen soil particles but also compact the soil surface and produce a crust (Moore and Singer 1990). The former process is more common early in a rainfall event, whereas the latter process dominates later in the event. Shallow overland flow generally does not exert sufficient shear stress on a soil surface to detach soil particles. However, where the soil is highly erodible and/or overland flow becomes concentrated along particular flow paths, the depth and velocity of flow may increase to the point where flow detachment dominates raindrop detachment, leading to the formation of rills and gullies. This is specifically the situation in the shrubland where shrub mounds divert overland flow and concentrate it in intershrub areas.

Sedigraphs of Simulated Runoff Events

Graphs of sediment concentration against time since the start of rain (hereafter called sedigraphs) for the rainfall simulation experiments suggest that sediment transport by overland flow on the

Summerford bajada is generally detachment-limited. Where animal digging is limited, sedigraphs are usually monotonically decreasing (figure 7-7).

This form is attributed to a reduction in the availability of detached sediment as the flow event proceeds. At the start of runoff, sediment concentration is high because the discharge is low and the flow is transporting loose sediment that has accumulated on the ground surface since the last event or that has been detached by rainfall prior to runoff. As discharge increases, the availability of detached sediment decreases, and the sedigraph declines monotonically (Neave and Abrahams 2002).

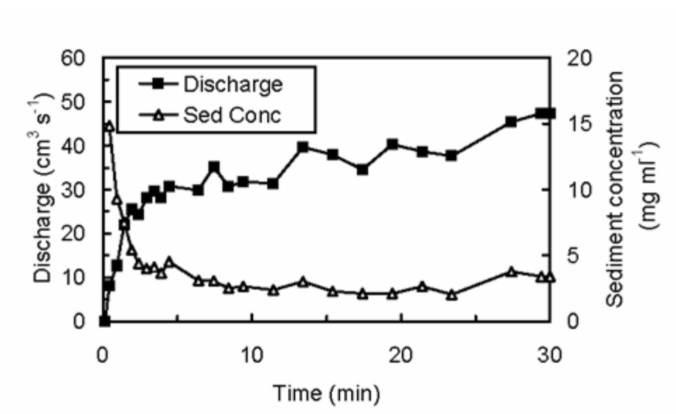

Fig. 7-7. Hydrograph (discharge) and sedigraph (sed. conc.) for a 30-min simulated rainstorm at target intensity of 144 mm h^{-1} on a runoff plot with little animal disturbances of soil surface.

In contrast, where animal digging has disturbed a significant proportion of the plot surface, the sedigraph may be almost any shape depending on the severity and distribution of the disturbances over the plot surface. Monotonically increasing, convex-upward, and oscillating

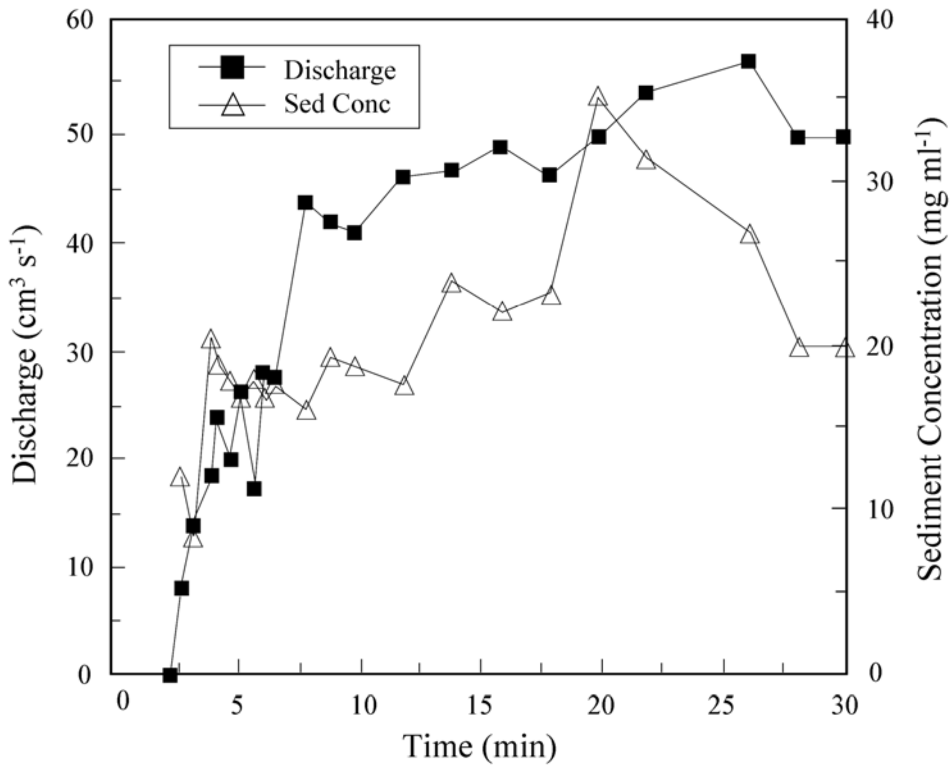

Fig. 7-8. Hydrograph (discharge) and sedigraph (sed. conc.) for a 30-min simulated rainstorm at target intensity of 144 mm/h on a runoff plot with extensive animal disturbance of soil surface over its upper zone.

sedigraphs are all common (figure 7-8). These shapes reflect the time it takes the flow to transport loose sediment from the various disturbance sites within the plot to the plot outlet. Thus both the shape of the sedigraph and the rate of sediment transport appear to be determined by the availability of detached sediment rather than the transport capacity of the flow, and the availability of such sediment are strongly influenced by animal disturbance of the soil surface (Neave and Abrahams 2002).

Controls

There is an extensive body of literature (reviewed by Weltz et al. 1998) on the controls of soil erosion and sediment yield on rangeland hill slopes. The principal controls of sediment yield are generally the same as those of runoff (already discussed): namely, plant and surface cover variables (standing biomass, life form class, canopy cover, and ground cover) and soil properties (bulk density, soil texture, soil organic carbon, and aggregate stability). Although the general character of these controls is similar from place to place, there are often important differences in detail. Rainfall simulation provides a powerful method not only for identifying these controls but also for investigating the pathways whereby they affect sediment yield.

Sediment yield, S_Y (kg/m^2), from a 30-min simulated rainfall experiment is equal to the product of water yield, W_Y (m), and sediment concentration, S_C (kg/m^3). Thus, the factors controlling S_Y may be thought of as acting through W_Y and/or S_C. The controls of W_Y were investigated earlier, and the findings are incorporated into figure 7-9. This figure depicts a causal model based on regression analyses of data obtained from the rainfall simulation experiments. The purpose of the model is to identify the surface properties controlling S_Y. The properties considered in the analysis are gravel cover, *percentG* (particle diameter > 2 mm); fines cover, *percentF*; ground vegetation cover, *percentV*; litter cover, *percentL*; the percentage of the surface disturbed by animals, P_A; and the mean diameter of the disturbances, D_A (mm). In figure 7-9 (1) only correlations that are significant at the 0.10 level are represented by arrows, (2) the arrowhead signals the direction of causality, (3) the strength of the causal relation is indicated by the standardized regression (beta) coefficient beside each arrow, (4) because $S_Y = W_Y S_C$, a

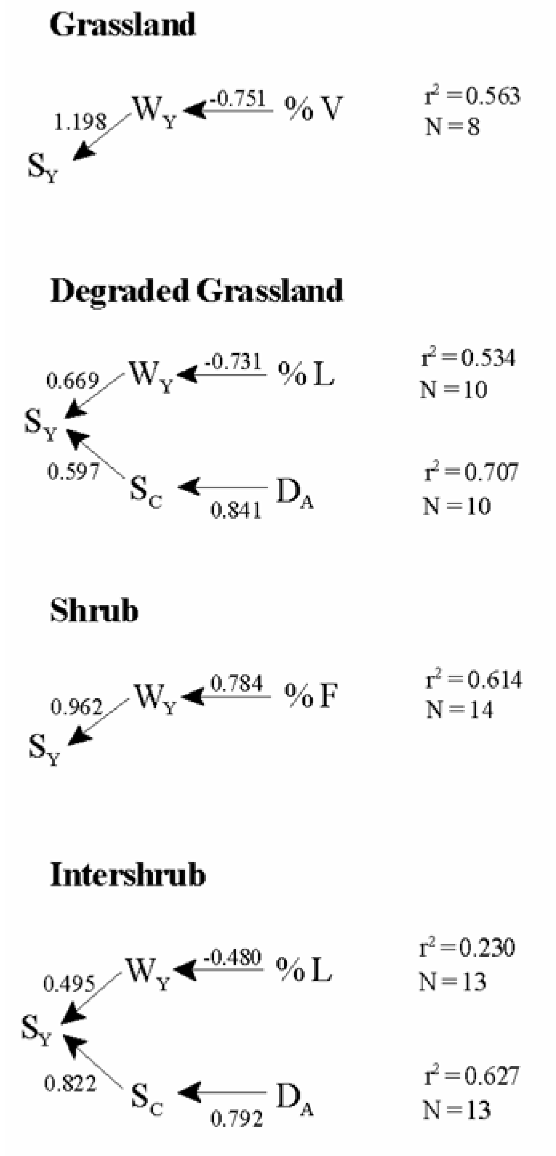

Fig. 7-9. Causal diagrams showing how surface properties control sediment yield (S_Y) through water yield (W_Y) and sediment concentration (S_C). The surface properties are vegetation cover (*%V*), litter cover (*%L*), fines cover (*%F*), and mean diameter of the animal disturbances (D_A). The numbers beside the arrows are standardized partial regression (beta) coefficients. All coefficients are significant at the 0.10 level. *N* is the sample size and r^2 is the coefficient of determination.

regression of S_Y against W_Y and S_C always gives r^2 = 1, and (5) the r^2 values for the relations between either W_Y or S_C and the surface properties are presented on the right-hand side.

Figure 7-9 shows that surface properties affect S_Y via their effect on W_Y in all cover types. In the grassland and shrub cover types this is the only way surface properties influence S_Y, because S_Y is independent of S_C. In contrast, in the intershrub and degraded grassland cover types, S_Y is related to S_C, which in turn is controlled by D_A. The positive correlations between D_A and S_C and between S_C and S_Y reflect the strong influence of animal digging on the movement of sediment in these two cover types (Neave and Abrahams 2001).

Rainfall Duration

The rainfall simulation experiments on which figure 7-9 is based were run at a target intensity of 144 mm/h for 30 min. Such a storm has a recurrence interval in excess of 100 years. An intensity of 144 mm/h is not unusual, but it is unusual for this intensity to persist for 30 min. The data were therefore examined to ascertain whether the relations displayed in figure 7-9 hold for shorter durations. The analyses revealed that all the significant relations in figure 7-9 are established after 15 min of rainfall and that some relations were established even earlier. The relations were weaker for the 5- and 10-min durations because runoff begins at different times on different plots, and the time to runoff has a major effect on the water and sediment yields during the first few minutes of a storm (Neave and Abrahams 2001).

Natural Runoff Events

Sediment yields obtained from the rainfall simulation experiments cannot be used to estimate annual sediment yields because the simulations were performed at a single intensity and duration, whereas natural rainfalls vary in intensity and duration. T. J. Ward (unpublished data) measured sediment loss from inter-rill areas during natural rainfall events. Because his data represent the rainfall regime, they may be used to calculate mean annual sediment yields for the grassland and shrubland. For this calculation, it was necessary to combine the data from the high-cover and low-cover plots in each community, and this in turn required that each plot type be assigned a weight. Based on the assumption that half the grassland has high cover and half low cover, each plot type was assigned a weight of 0.50. In the shrubland, the high-cover and low-cover plots correspond to shrub and intershrub areas, respectively. Because shrub canopies occupy about 38% of the shrubland surface (Schlesinger et al. 1999, 2000), the high-cover plots were assigned a weight of 0.38, and the low-cover plots had a weight of 0.62.

The mean annual sediment yield and volume-weighted mean sediment concentration are highest for the low-cover shrubland (intershrub areas) and lowest for the high-cover grassland. The differences are large, with the sediment yield for the low-cover shrubland being 7.9 times that for the high-cover shrubland. The sediment yield and the sediment concentration are also higher for the shrubland than for the grassland, with the sediment yield for the former exceeding that for the latter by a factor of 2.7. The mean annual runoff for the shrubland is 3.4 times that for the grassland, and the volume-weighted mean sediment concentration for the shrubland is 1.4 times that for the grassland. Thus the higher sediment yields in the shrubland are due to both higher runoffs and higher sediment concentrations, with the runoff having a larger effect than the sediment concentration.

Nutrients

Our hypothesis for the desertification of piedmont grasslands in the Jornada Basin suggests that as the plant cover in grasslands declines, greater rates of hill slope erosion remove nutrients from exposed soils, thereby reinforcing the development of resource islands under invading shrubs. To test this hypothesis, we measured the nutrient concentrations in runoff during 24 rainfall-simulation experiments on areas of black grama grassland and creosotebush shrubland (*Larrea tridentata*) on the Summerford bajada (Schlesinger et al. 1999). The objective was to compare the runoff of nitrogen (N) and phosphorus (P) from these habitats to assess whether greater losses of soil nutrients are associated with the invasion of grasslands by shrubs.

Volume-weighted mean concentrations of total dissolved N in runoff (total N loss divided by total water loss) were 1.72 mg/L, l.44 mg/L, and 0.55 mg/L for the grassland, shrub, and intershrub plots, respectively. Weighted by the average cover of shrub (38%) and intershrub (62%) areas on the landscape, the mean nitrogen concentration was 0.77 mg/L in the runoff from shrublands. Thus the concentration of total dissolved N in the runoff from grasslands was 2.23 times greater than that from the shrubland. Volume-weighted mean concentrations of dissolved organic nitrogen (DON) were 1.00 mg/L, 0.87 mg/L, and 0.41 mg/L for the grassland, shrub, and intershrub plots, respectively. Weighted by the average cover of shrub and intershrub areas, the mean concentration of DON in the runoff from shrublands was 0.52 mg/L. Thus, the DON concentration in the runoff of grasslands was l.9 times greater than in the runoff from shrublands.

For grassland and shrub plots, N yield was always more highly correlated with water yield than with N concentration, whereas the reverse was true for the intershrub plots. The standard deviation of water yield was always greater than the standard deviation of N concentration for grassland and shrub plots, but less than the standard deviations of these variables on intershrub plots. This suggests that intershrub plots were similar in their ability to generate runoff but different in their ability to supply N compared to grassland and shrub cover types. Given that intershrub plots were virtually devoid of ground vegetation and litter, and whereas the grassland and shrub plots had varying covers of plant matter, the greater hydrological uniformity of the intershrub plots is not surprising. It is less obvious, however, why the intershrub plots were more variable than the grassland and shrub plots in their supply of N in general and of organic N in particular. There were no significant correlations between our measures of surface properties in these plots and their yield of runoff or N.

Bolton et al. (1991) suggested that a useful statistic for comparing nutrient losses in arid lands is the volume-weighted mean concentration (e.g., mg N/¬) divided by 100, which is equivalent to the loss of N (kg/ha) per ml of runoff. Over a 6-year period, 1989–94, an average of 14.6 mm/yr of runoff (6% of incident precipitation) was measured on eight 2-m by 2-m runoff plots in two grasslands of the Jornada Basin. Using the volume-weighted mean concentration of 1.72 mg N/L for total dissolved N in the runoff from grasslands, nitrogen losses were calculated to be 0.25 kg/ha/yr.

To estimate the annual loss of N from shrublands, the volume-weighted mean concentrations of total dissolved N in runoff (1.44 mg N/L for shrub plots and 0.55 mg N/L for intershrub plots) were weighted by the runoff and proportional land area of shrubs (38%) and intershrub areas (62%) and then multiplied by a runoff estimate of 56.2 mm/yr (18% of incident precipitation) determined on four 2-m by 2-m plots monitored in creosotebush shrubland during the same 6-year period as in the grasslands. The calculated N loss was 0.43 kg/ha/yr. The higher loss of dissolved N from shrublands than from grasslands stems from the 3.8 times greater runoff measured in shrublands during the long-term field studies.

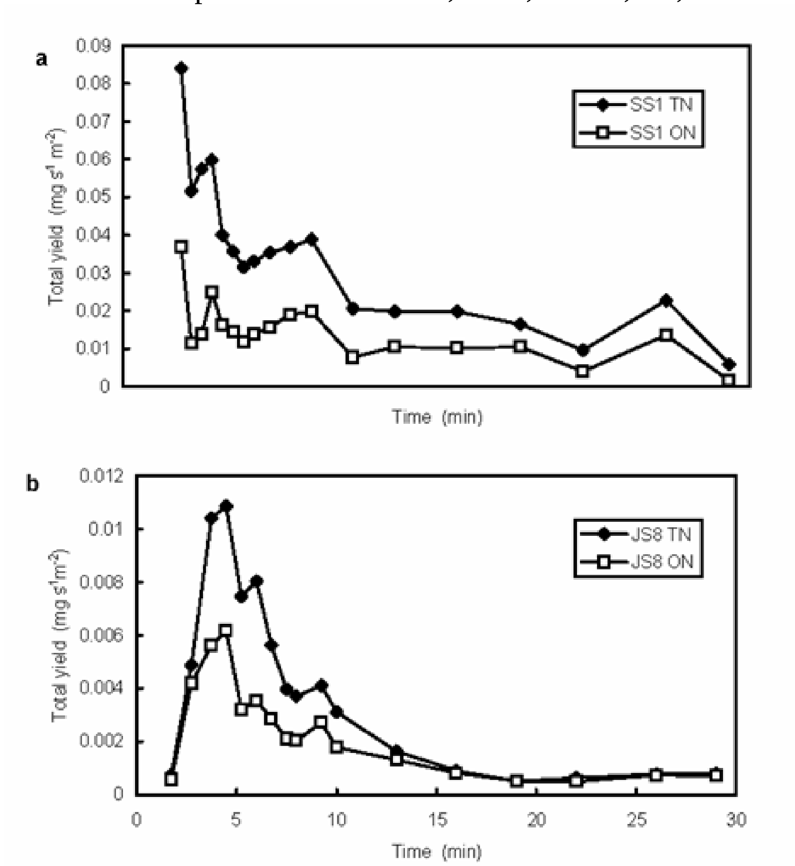

Fig. 7-10. Yields of organic nitrogen (ON) and total dissolved nitrogen (TN) in discharge as a function of time since the start of simulated rainfall from grassland (a) and shrubland (b) plots.

Despite the sparseness of arid land vegetation, DON was greater than 50% of the total dissolved N measured in the runoff from grassland and shrub plots, accounting for nearly 70% of the N lost from the barren soils of the intershrub plots. The total yield of N during each rainfall simulation declined monotonically (figure 7-10), suggesting that the decline in the concentration of N over time was not simply due to dilution by the increasing runoff but to depletion of the pool of available N in the soil.

The decline was greater for dissolved inorganic forms of nitrogen (NH_4 and NO_3) than for DON, so DON became an increasing fraction of the total N yield as duration of runoff increased. These high concentrations of DON may be seasonal; the rainfall simulation experiments were performed at the end of the dry season, when a large quantity of soluble organic N compounds may have accumulated undecomposed in the soil.

The nutrient losses in runoff during the rainfall simulation experiments were compared to the losses of dissolved nutrients (N, P, K, Ca, Mg, Na, Cl, and SO_4) in runoff measured during natural runoff events of varying intensity and duration on grassland and shrubland plots in the Jornada Basin (Schlesinger et al. 2000). Across all plots at each site, runoff was logarithmically related to precipitation volume, with r^2 ranging from 0.44 to 0.48 (figures 7-11a and 7-11b). An analysis of variance showed that the mean slope of this relationship, calculated from the slope of the regressions for the individual runoff plots in each area ($N = 4$), was not different between grassland and shrubland plots. However, the intercepts of the relationship were lower for both grasslands than for the shrubland, suggesting that runoff commenced at a lower threshold of storm size in the shrubland than in the grasslands. The annual runoff coefficient (total depth of runoff expressed as a percentage of the total depth of precipitation received) averaged 19% in the creosotebush shrubland and 6% in the grasslands.

Within each area, plant cover did not significantly affect the slope of the relationship between runoff and precipitation, although the difference between high- and low-cover plots is nearly significant in the grassland. The volumetric runoff coefficient averaged 8.5% in low-cover plots and 4.1% in high-cover plots during a 5.5-year period of collections in the grasslands.

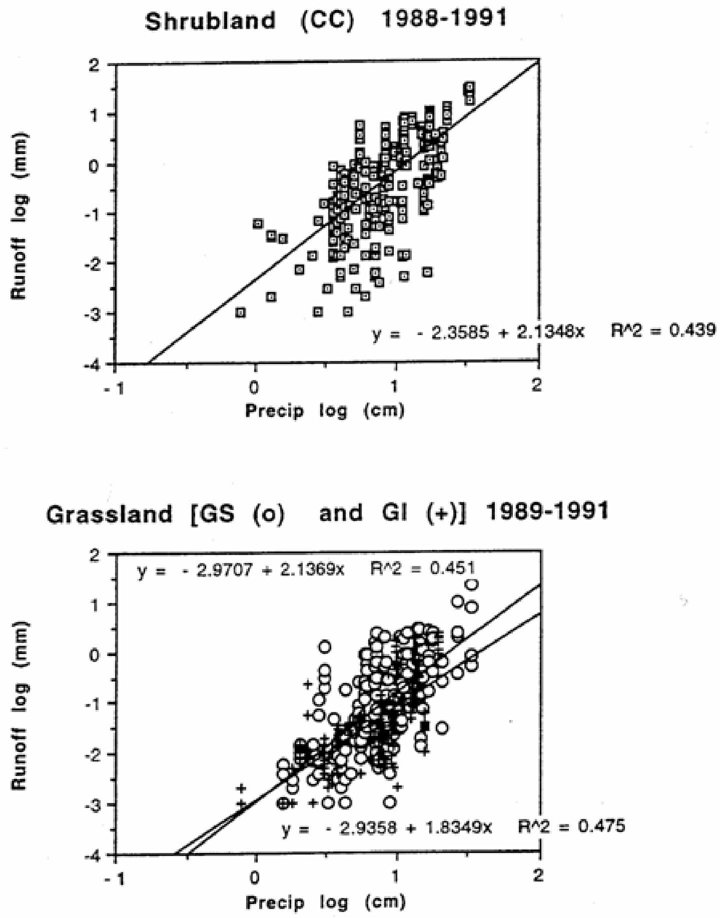

Fig. 7-11. Total runoff during natural rainfall events from plots in shrubland and grassland as a function of total rainfall during the event. CC denotes creosotebush *(Larrea tridentata)* shrubland on the Summerford bajada, GS denotes grassland on the Summerford bajada, and GI grassland about 10 km to the north.

During the 7-year record in the creosotebush shrubland, the annual runoff coefficient was 16.4% in high-cover plots versus 20.8% in low-cover (intershrub) plots. As in the rainfall simulation experiments, the data from the field plots show that a loss of grass cover leads to greater runoff from dryland ecosystems (see Abrahams et al. 1995; Gutierrez and Hernandez 1996; Castillo et al. 1997). Discharge commences earlier in the shrubland than the grassland. Specifically, an average of 2.72 mm of rain is required to initiate runoff in the shrubland, whereas 3.25 mm is required in the grassland. Total discharge during a storm increases with the volume of rainfall received, but the slopes of these relationships differ little between the grassland and shrubland (figure 7-11) or between high- and low-cover plots (figure 7-11b).

The concentrations of dissolved constituents declined with increasing runoff volume in all habitats. The best relationships between concentration and volume were always logarithmic, reflecting a rapid dilution of dissolved constituents with increasing discharge (figures 7-12a–c). The yield of dissolved constituents in each runoff event was calculated by multiplying the concentration (mg/L) by the runoff volume (L). Annual losses of dissolved forms of plant nutrients in runoff were always higher in the creosotebush shrubland than in the grasslands. Losses of total dissolved nitrogen ranged from 0.28 to 0.41 kg/ha/yr in the shrubland (figure 7-12a) versus 0.11–0.21 kg/ha/yr in the grassland plots (figures 7-12b and 7-12c). DON made up 10–30% of the loss of total dissolved N in each habitat. Higher overall discharge, rather than higher nutrient concentrations in runoff waters, accounts for the greater losses of nutrients from shrublands. The weighted mean concentration of total dissolved N was 0.71 mg N/L in the creosotebush shrubland and 1.39–3.24 mg N/L in the grasslands. These concentrations compare favorably to those measured in shrubland and grasslands during the rainfall simulation

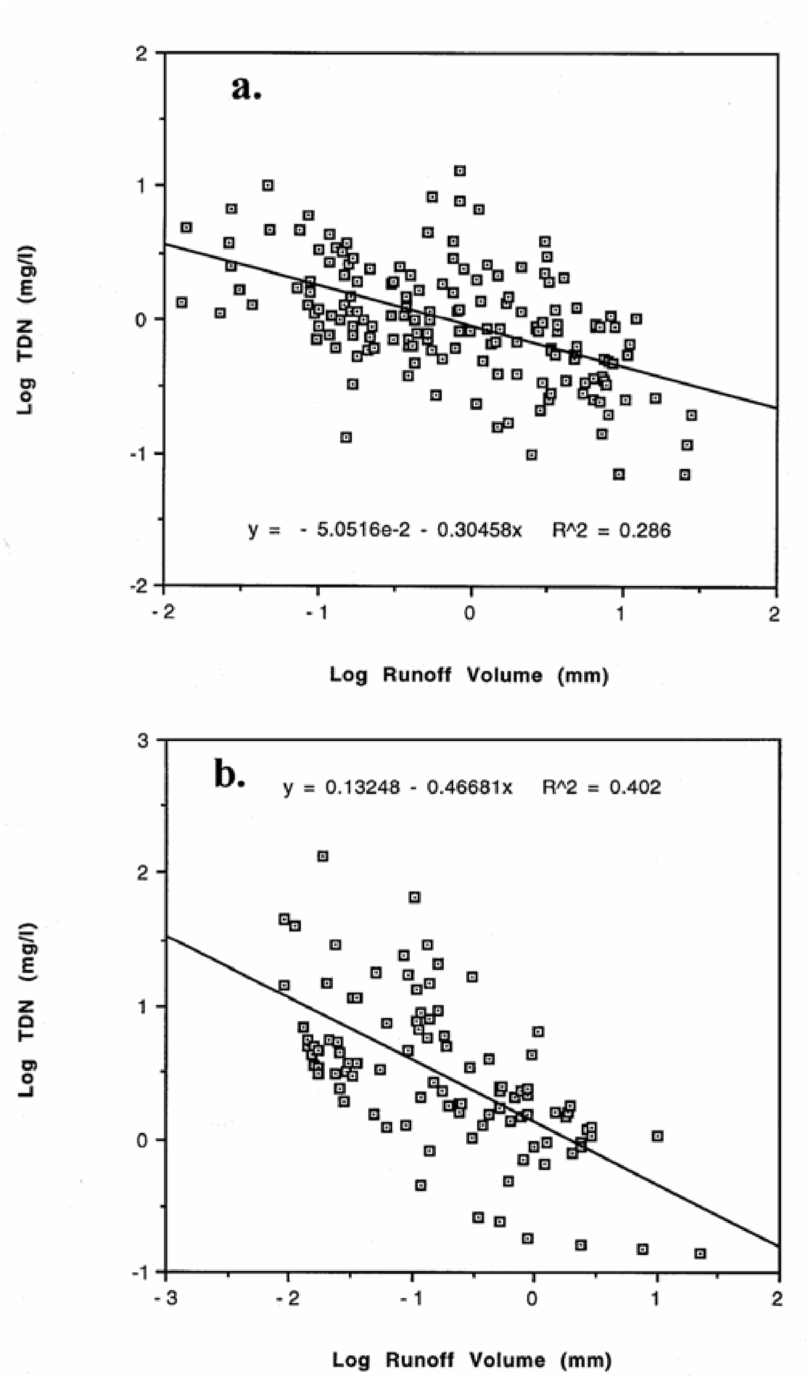

Fig. 7-11. Total runoff during natural rainfall events from plots in shrubland and grassland as a function of total rainfall during the event. CC denotes creosotebush *(Larrea tridentata)* shrubland on the Summerford bajada, GS denotes grassland on the Summerford bajada, and GI grassland about 10 km to the north.

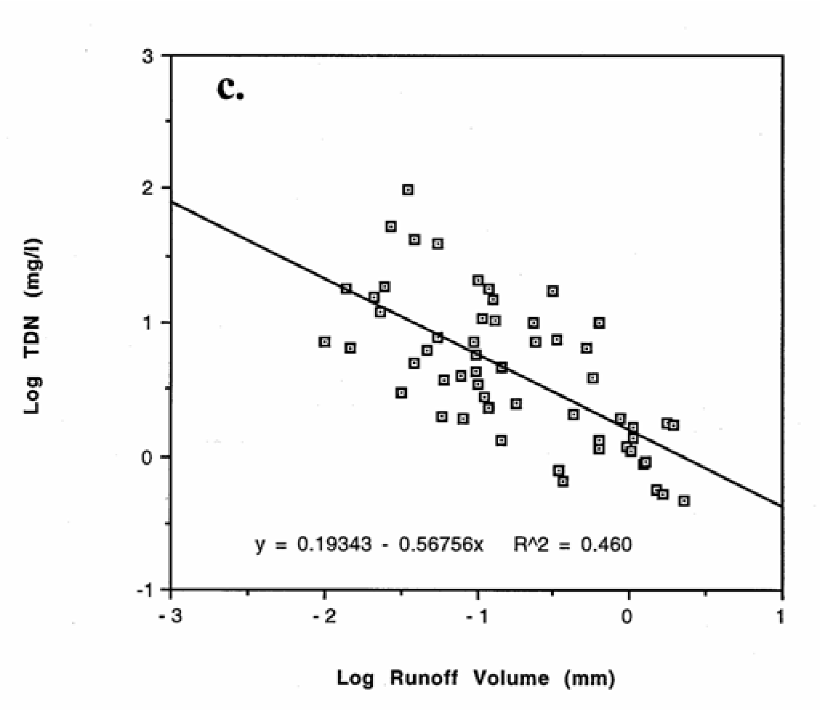

experiments. In both the shrubland and grassland plots, the losses of N found were less than those estimated from the rainfall simulation experiments (0.43 and 0.25 kg/ha/yr, respectively; Schlesinger et al. 1999). The mean runoff for 1988–91 was below the long-term average (1989–94) that we used to make a long-term extrapolation of N yield from the rainfall simulation experiments. Although the mean N losses in runoff are greater in the shrubland (0.33 kg ha/yr) than in the grasslands (0.12 and 0.19 kg/ha/yr), the transport of dissolved N compounds in runoff cannot be wholly responsible for the depletion of soil N that is associated with desertification in this region (Schlesinger et al. 1996; Kieft et al. 1998). The N losses in runoff are lower than the inputs in atmospheric deposition; so all habitats show a net gain of soil N if one considers only atmospheric deposition and runoff.

Conclusions

This chapter summarizes our characterizations of the movement of water, sediment, and nutrients across the Summerford bajada. The lateral transfer of water and materials is accomplished by both channelized flows in rills and washes and unchannelized flows over inter-rill surfaces. The focus of the work has been on inter-rill flows, which are strongly influenced by raindrop impact. Rainfall simulation is a powerful tool for investigating such flows, and we have made extensive use of it in these characterizations. Analyses of rainfall simulations (including unpublished data provided by Ward) and natural rainfall events have led to the following findings.

1. Creosotebush shrubs and the areas (interspaces) between them are hydrologically very different. In particular, under equilibrium conditions interception by the shrub canopy causes the mean kinetic energy of the subcanopy rainfall to decline by 30%, which reduces surface sealing and contributes to the formation of shrub mounds by differential splash. These mounds, which are the topographic representation of a resource island, divert overland flow and concentrate it in intershrub areas, where flow detachment lowers the surface and may ultimately scour a rill. Stem flow is another process contributing to the formation of resource islands. An average of one-sixth of the rainfall intercepted by the canopy is funnelled to the base of the shrub. Direct and released throughfall also contribute water to resource islands, and the disposition of this water (i.e., infiltration and surface runoff) is controlled by the density of subcanopy vegetation. On plots devoid of such vegetation, runoff averages 77% of rainfall intensity. In contrast, where there is dense subcanopy vegetation, this proportion ranges from 0 to 16% as rainfall intensity increases from 0 to 20 cm/h.

2. Whereas runoff from shrub areas is strongly influenced by subcanopy vegetation, runoff from intershrub areas is largely controlled by surface crusting. Biological and physical crusts coexist, and their effects are generally difficult to separate. Physical crusts, however, are more dynamic than biological crusts: They can form during a single storm and be effectively destroyed in a matter of weeks by animal activity. As a result of crusting, runoff from intershrub areas is about three times that from shrub areas, and runoff from degraded grassland is about three times that from grassland.

3. Runoff coefficients for the grassland and shrubland are 6% and 19%, respectively, whereas maximum runoff in the shrubland is 2.2 times that in the grassland. These differences between grassland and shrubland are largely attributed to the fact that almost two-thirds of the shrubland community consists of barren intershrub areas with crusted surfaces and low infiltration rates. Most runoff from the shrubland is generated in these intershrub areas and is largely confined to these areas as it flows downslope.

4. Rainfall simulation experiments demonstrate that animal digging and scratching, which are most pronounced in the interspaces between shrubs and in the degraded grassland, have a major effect on sediment yields. Sediment yields from the shrubland are 2.7 times those from the grassland. Because the mean annual runoff for the shrubland is 3.4 times that of the grassland while the sediment concentration is only 1.4 times that for the grassland, it is evident that the higher sediment yields for the shrubland are due to both higher sediment concentrations and higher runoffs, with the higher runoffs having the greater effect.

5. The foregoing numbers suggest that as shrubland has replaced grassland on the Summerford bajada, intershrub areas have experienced greater rates of erosion, which have

removed nutrients and promoted the development of resource islands. Rainfall simulation experiments indicate that although the mean concentration of total dissolved N is lowest in bare intershrub areas and highest in grassland, total N yield is highest from intershrub areas and lowest from grassland due to the higher runoff from the intershrub areas. Surprisingly, in all three cover types, more than half the N transported in runoff is carried in dissolved organic compounds. Analyses of the data for natural rainfall events indicate that average nutrient losses from the shrubland is 0.33 kg/ha/yr, which is more than twice the value of 0.15 kg/ha/yr obtained for the grassland. Moreover, these data confirm that the greater nutrient losses from the shrubland are due to higher runoff rather than higher nutrient concentrations in runoff. These findings pertain to inter-rill areas, where runoff exceeds run-in and erosion processes dominate.